PROCEEDINGS A

royalsocietypublishing.org/journal/rspa

Research

Cite this article: Fan J, Yin Q, Xia C, Perc M. 2022 Epidemics on multilayer simplicial complexes. *Proc. R. Soc. A* **478**: 20220059. https://doi.org/10.1098/rspa.2022.0059

Received: 22 January 2022
Accepted: 31 March 2022

Subject Areas:
complexity

Keywords:
simplicial complexes, complex network, social contagion, epidemic spreading, nonlinear dynamics

Authors for correspondence:
Chengyi Xia
e-mail: xialooking@163.com
Matjaž Perc
e-mail: matjaz.perc@gmail.com

Epidemics on multilayer simplicial complexes

Junfeng Fan[1], Qian Yin[1], Chengyi Xia[1] and Matjaž Perc[2,3,4,5]

[1]Tianjin Key Laboratory of Intelligence Computing and Novel Software Technology, Tianjin University of Technology, Tianjin 300384, People's Republic of China
[2]Faculty of Natural Sciences and Mathematics, University of Maribor, Koroška cesta 160, 2000 Maribor, Slovenia
[3]Department of Medical Research, China Medical University Hospital, China Medical University, Taichung 404332, Taiwan
[4]Alma Mater Europaea, Slovenska ulica 17 2000 Maribor, Slovenia
[5]Complexity Science Hub Vienna, Josefstädterstraße 39, 1080 Vienna, Austria

MP, 0000-0002-3087-541X

Simplicial complexes describe the simple fact that in social networks a link can connect more than two individuals. As we show here, this has far-reaching consequences for epidemic spreading, in particular in the context of a multilayer network model, where one layer is a virtual social network and the other one is a physical contact network. The social network layer is responsible for the transmission of information via pairwise or higher order 2-simplex interactions among individuals, while the physical layer is responsible for the epidemic spreading. We use the microscopic Markov chain approach to derive the probability transition equations and to determine epidemic outbreak thresholds. We further support these results with Monte Carlo simulations, which are in good agreement, thus confirming the analytical tractability of the proposed model. We find that information transmission rates are frequently low when actual disease transmission rates in the physical network are low or medium, and we show that this can be mitigated effectively by introducing 2-simplex interactions in the social network. The relative ease of introducing higher-order interactions in virtual social networks means that this could be exploited to inhibit epidemic outbreaks.

THE ROYAL SOCIETY PUBLISHING

1. Introduction

Over the past two decades, real-world systems are often modelled as complex networks [1–4], where nodes denote entities within the systems, and links represent the interactions among them. Most recently, many complex systems have been described by multiple interdependent networks or multilayer networks [5–16]. As a typical example, there exists an intricate interplay between the power system and communication network [6], where, on the one hand, the basic function of the communication system requires a proper power supply from the electrical system to keep its running; on the other hand, only when the communication system is working properly can the electricity generated by the power system be transferred continuously to the places where it is needed. Similar interdependent networks include transportation systems, social networks, ecosystems and so on [11,12]. Meanwhile, the dynamics taking place on interdependent or multilayer networks receive a great deal of concern, especially for the epidemic spreading behaviour on multilayer networks [17–22]. For instance, Granell *et al*. [20] proposed a two-layered network model, in which the upper one is a virtual contact layer, used to describe information propagation, and nodes in this layer have two possible states: aware (A) or unaware (U); while the lower one is used to depict the physical contact layer, where disease contagion takes place, and nodes in this layer have two possible states: susceptible (S) or infectious (I). It was clearly found that the network structure and awareness diffusion can make an impact on the outbreak threshold of infectious diseases. Also, information transmission of infectious diseases is helpful to suppress its spreading, reduce its incidence and even contribute to its eradication [20–23].

However, regarding the propagation of information or behaviour on networks, previous works have essentially been investigated on the basis of pairwise interactions, which neglect high-order or non-pairwise interactions among nodes. In fact, from human communication [24–28] to animals' brains [29–31] and ecosystems [32–34], interactions may often occur among clusters of three or more nodes, which cannot be described simply by the pairwise interactions between two nodes [23,35–50]. As an example, Iacopini *et al.* [27] adopted random simplicial complexes to construct single-layer networks that simulate the epidemic spreading among individuals. Based on the mean field approach, they found that their new method can capture the underlying mechanism and effect of higher-order topology during social contagion, and a bi-stable state of infective density was discovered, which is related to the initial density of infectious individuals. By studying the gaming behaviour on the uniform hypergraph, [28] found that the presence of hubs and their interaction with groups of different sizes will affect the evolution of cooperation. By introducing high-order structures in graph theory, such as clusters and holes, into the neural network models of the human brain, [30] found that clusters and holes in the cerebral cortex play an important role in human perspective and cognitive function. They also discovered that holes are closely related to the patterns of information transmission in the brain. In addition, [33] found that high-order interactions of species determine the diversity of natural ecosystems.

In order to further reveal some new phenomena that may arise from the introduction of random simplicial complexes for the information transmission coupled with epidemic propagation, we propose a new two-layer model to explore the impact of high-order interactions in information diffusion on disease spreading. Here, the upper layer represents the virtual layer, which is used to denote information diffusion among individuals, and random simplicial complexes are used to construct the corresponding network [27]. The lower network stands for the physical layer, which is adopted to depict the epidemic spreading among people, and the Erdös–Rényi (ER) random graph [51] is used to create its topology. It is found through extensive simulations that, at the steady state, the densities of infectious nodes obtained through the microscopic Markov chain (MMC) approach closely agree with ones obtained through Monte Carlo (MC) simulations, and the density of infectious individuals decreases as the information transmission rate from 2-simplex increases. It is also discovered that random simplicial complexes can affect the outbreak threshold of the disease, which demonstrates that the network constructed with random simplicial complexes in the upper layer has a potential impact on the contagion dynamics of the entire system.

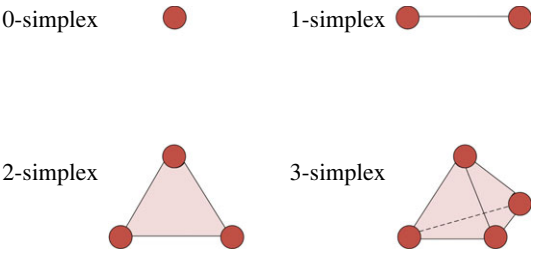

Figure 1. Illustrative examples of the 0, 1, 2 and 3-simplex. The 2-simplex includes not only the tree nodes and tree edges, but also the whole area they surround. Similarly, the 3-simplex includes the four nodes, six edges and the three-dimensional space they surround. (Online version in colour.)

The remaining sections are organized as follows. In §2, we firstly introduce the two-layer network model and use MMC approach to derive the probability transition equations to analyse the outbreak threshold of the epidemics. Then, §3 presents the numerical simulations obtained by MC simulations and analytical results from MMC, respectively. Lastly, we end the paper with some concluding remarks in §4.

2. Methods and models

(a) Simplicial complex

Before introducing our model, let us recall some basic concepts about simplicial complexes. A k-simplex s is a convex polytope that consists of $k+1$ vertices. For a given set of vertices V, with $|V| = N$, a simplicial complex K is a collection of simplices, which means that if simplex $s \in K$, then all the subsimplices $v \subset s$ built from s are also contained in K. In general, we call nodes as 0-simplices, links as 1-simplices. One 2-simplex is a 'full' triangle composed of not only three nodes and three links, but also the whole area they surround. One 3-simplex is the tetrahedral, and so on. Several typical simplices are shown in figure 1.

(b) Two-layer network model

In this paper, a two-layer network model is used to characterize the coupling propagation between epidemics and related information. On the one hand, the upper layer depicts the information spread on social networks, such as Facebook, Twitter, WeChat and other social platforms. However, unlike previous works, the upper layer network in this paper is constructed with random simplicial complexes; that is, not only the information propagation of pairwise interactions is considered, but the additional information contagion that may be caused by simplicial complexes is also pondered.

On the other hand, the lower layer denotes the epidemic spreading behaviour within the real-world social networks, and the classical SIS model is used to describe the epidemic spreading processes in the lower layer, in which nodes may be in two possible states: infectious (I) or susceptible (S). In the model, at each time step, S state nodes are infected by infective neighbours and become I state with the probability β. Meanwhile, the infectious nodes recover and switch into S state with probability μ.

Each node in the upper network is just mapped onto one node in the lower network, which means that every node in the network will be influenced by both information and infectious diseases. At the same time, it is assumed that the whole network is undirected and unweighted, as shown in figure 2.

In the upper layer, nodes may be in two distinct states: unaware (U) or aware (A) of the epidemics. At each time step, information propagation is divided into two stages: the first

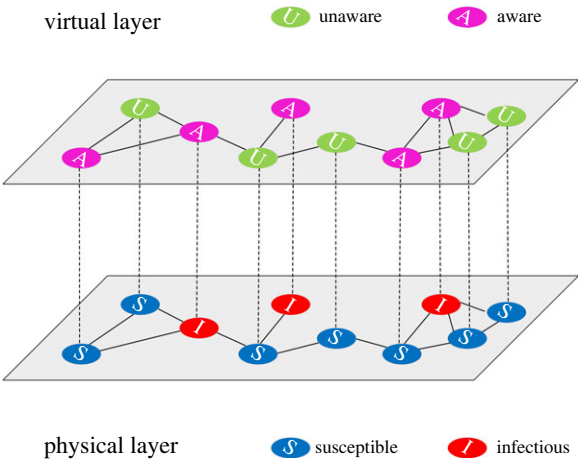

Figure 2. The proposed two-layer transmission model in this paper, in which the upper layer simulates the spread of information about the disease, while the lower layer describes the epidemic propagation. The dotted lines between upper and lower layers mean that nodes are matched one by one. Meanwhile, the network is undirected and unweighted. (Online version in colour.)

one is to propagate news or information related with the disease through direct links, within which unaware nodes receive information from aware neighbouring nodes and become aware with probability λ. Aware nodes may lose the related information and become unaware with probability δ. The second stage represents the effect of simplicial complexes (only the impact of 2-simplex is considered here), for example, three nodes i, j, k form 2-simplex, if nodes k and j are in A state and node i is in U state, then node i will be again infected by the rate λ^* through 2-simplex. Thus, U state nodes may become A through the pairwise or 2-simplex interactions with their neighbours, which are shown in figure 3.

Among them, aware nodes may take protective measures to reduce their risk of being infected since they are aware of the spreading of epidemics, while the unaware nodes would not take any protective measures when confronted with epidemics. Using β^A to represent the probability of aware nodes being infected and β^U to denote the probability of unaware nodes being infected, it is hypothesized that $\beta^A = \gamma\beta^U$, where $0 \leq \gamma \leq 1$ means that the probability for A nodes to be infected is lower than that of the U node. In particular, if $\gamma = 0$, it means that nodes in the A state will not be infected once they are aware. After individuals in the physical layer are infected, they will be self-aware with the probability 1 and their corresponding state on the virtual layer will spontaneously switch to A. Taking together, the individual states on two layers will be combined and classified as three classes: AI, AS and US. Note that the UI state is absent since the infectious individuals will be assumed to immediately become aware of the information of infectious diseases and spontaneously become AI.

It is notable that the upper layer network in the proposed model is constructed with 2-simplicial complexes [27], which can be divided into the following three steps:

(i) Initialize the number of nodes in the network to be N. Let k_1 denote the average degree of nodes in the upper network, k_2 be the amount of 2-simplices within which each node may locate.
(ii) Generate an ER-random network with the linking probability p_1 $(0 < p_1 < 1)$, which means the probability of any two nodes to be connected within the network. Then, the average degree of nodes in the network is $(N-1)p_1$ at this time.
(iii) Let p_2 $(0 < p_2 < 1)$ stand for the probability of forming a 2-simplex through any three nodes i, j, k. After generating 2-simplices for all nodes in the network with the probability

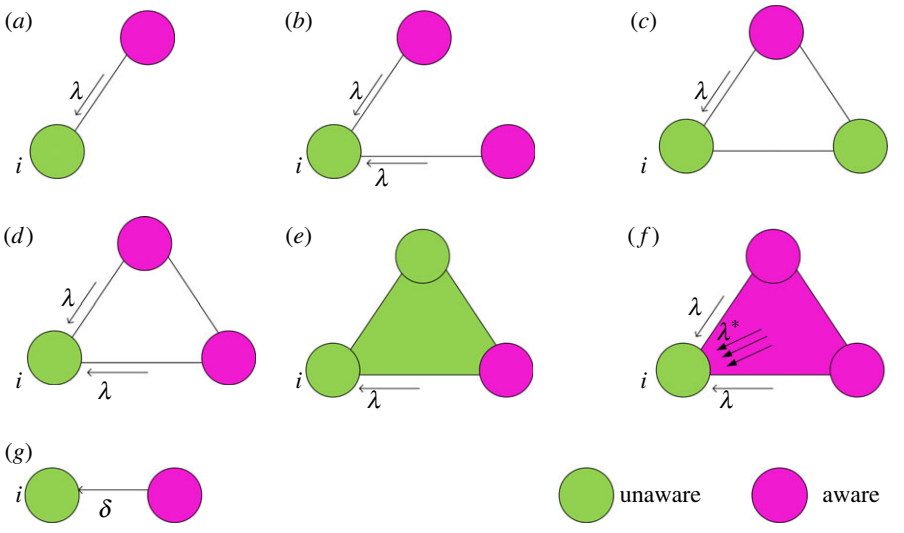

Figure 3. Panels (*a*)–(*f*) denote different cases that *U* state node *i* may be notified by its *A* state neighbour nodes. Panel (*a*) is a 1-simplex (link) and node *i* is connected to an *A* state node, so node *i* may be notified to become *A* state with λ probability at each time step. In panel (*b*), node *i* is connected to two *A* state nodes. Panel (*d*) denotes three 1-simplices, and since they do not form a 2-simplex (missing the face of the triangular enclosure), each edge connected to node *i* denotes node *i* may be notified to become *A* state at each time step with probability λ. In panel (*e*), they form a 2-simplex, but there is only one node in *A* state, which does not meet the information dissemination conditions of the 2-simplex. Panel (*f*) denotes a 2-simplex, at each time step, node *i* not only notified by each *A* state node and become *A* state with probability λ, but also may become *A* state with probability λ^* under the influence of the whole 2-simplex. In addition, nodes in *A* state may become *U* state with probability δ for loss of information at each time step, which is shown in panel (*g*). (Online version in colour.)

p_2, the newly generated edges will be added into the ER-random network obtained in the second step. Thus, $k_2 = (N-1)(N-2)p_2/2$.

It needs to be noted that the average degree of the nodes of ER-random network generated at step (ii) will be expanded at step (iii), and thus the increases in the average degree caused by the 2-simplex need to be analysed in detail.

Firstly, supposing that there is no edge between *i* and *j*, *i* and *k*, it happens with the probability $(1-p_1)^2$. After linking *i* and *j*, *i* and *k*, the average degree of nodes in the ER-random network generated at step (ii) will be increased by 2. Secondly, assuming that there is no edge between *i* and *j*, but there is an edge between *i* and *k*. This situation happens with probability $(1-p_1)p_1$. After linking *i* and *j*, the average degree of nodes in the ER-random network will be increased by 1. Lastly, if there is no edge between *i* and *k*, but there is an edge between *i* and *j*, the variation of the average degree is similar to that in the second case.

Summing up, $2(1-p_1)^2 + (1-p_1)p_1 + (1-p_1)p_1 = 2(1-p_1)$ will be added into the average degree of nodes in the ER-random network by a 2-simplex. Then, $k_1 = (N-1)p_1 + 2(1-p_1)k_2$. By using the algebraic equivalence transformation, p_1 and p_2 can be calculated as follows:

$$\left.\begin{aligned} p_1 &= \frac{k_1 - 2k_2}{(N-1) - 2k_2} \\ \text{and} \quad p_2 &= \frac{2k_2}{(N-1)(N-2)} \end{aligned}\right\} \tag{2.1}$$

(c) Analytical results based on the MMC approach

Let $[a_{ij}]$ and $[b_{ij}]$ denote the adjacency matrices of the upper and lower layer networks, respectively. $p_i^{AI}(t)$, $p_i^{AS}(t)$ and $p_i^{US}(t)$ mean the probabilities of node i being at the state of AI, AS and US at time t, respectively. Meanwhile, $q_i^A(t)$ represents the probability of node i not being infected by any neighbour if node i is aware at time t, and $q_i^U(t)$ is used to denote the probability of node i not being infected by any neighbour at time t if i is unaware. $r_i(t)$ is assumed to be the probability of node i not being informed by any neighbour at time t which can be calculated by multiplying $r_i^1(t)$ and $r_i^2(t)$. Here, $r_i^1(t)$ denotes the probability that node i is not informed by the pairwise interaction of its neighbours at time t, and $r_i^2(t)$ stands for the probability that node i is not informed by the 2-simplex interaction of its neighbours at time t. According to the aforementioned definitions and assumptions, the above quantities can be computed as follows:

$$\left.\begin{aligned} q_i^A(t) &= \prod_j (1 - b_{ji} p_j^{AI}(t)\beta^A), \\ q_i^U(t) &= \prod_j (1 - b_{ji} p_j^{AI}(t)\beta^U), \\ r_i^1(t) &= \prod_j (1 - a_{ji} p_j^A(t)\lambda), \\ r_i^2(t) &= \prod_{c_i} (1 - c_{ijk} p_j^A(t) p_k^A(t)\lambda^*) \\ \text{and} \qquad r_i(t) &= r_i^1(t) r_i^2(t), \end{aligned}\right\} \tag{2.2}$$

where $p_j^A = p_j^{AI} + p_j^{AS}$. In the expression of $r_i^2(t)$, c_i indicates the number of 2-simplices around node i, c_{ijk} means whether these three nodes form a 2-simplex, and λ^* denotes the information transmission rate of the 2-simplex where node i is located, which can be further calculated by the following equation:

$$\lambda^* = \frac{\delta \lambda_\delta}{k_2}, \tag{2.3}$$

where λ_δ is the rescaled transmission parameter. Then, using equations above and the transition probability trees of each state shown in figure 4, the transition probabilities of all possible states in the proposed model can be obtained, which is shown in equation (2.4),

$$\left.\begin{aligned} p_i^{AI}(t+1) &= p_i^{AS}(t)[\delta(1 - q_i^U(t)) + (1-\delta)(1 - q_i^A(t))] + p_i^{AI}(t)(1-\mu) \\ &\quad + p_i^{US}(t)[(1 - r_i(t)(1 - q_i^A(t)) + r_i(t)(1 - q_i^U(t))] \\ p_i^{US}(t+1) &= p_i^{AS}(t)\delta q_i^U(t) + p_i^{AI}(t)\delta\mu + p_i^{US}(t) r_i(t) q_i^U(t) \\ \text{and} \qquad p_i^{AS}(t+1) &= p_i^{AS}(t)(1-\delta) q_i^A(t) + p_i^{AI}(t)(1-\delta)\mu + p_i^{US}(t)(1 - r_i(t) q_i^A(t)) \end{aligned}\right\} \tag{2.4}$$

As $t \to \infty$, the transmission of information and disease in the model will tend to be steady, and we can obtain the following steady-state equations:

$$\left.\begin{aligned} p_i^{AI}(t+1) &= p_i^{AI}(t) = p_i^{AI}, \\ p_i^{AS}(t+1) &= p_i^{AS}(t) = p_i^{AS} \\ \text{and} \qquad p_i^{US}(t+1) &= p_i^{US}(t) = p_i^{US}. \end{aligned}\right\} \tag{2.5}$$

As is well known, in the classical SIS epidemic model, if $\beta > \beta_c$, the contagion will diffuse broadly among individuals for a long time. Otherwise, the disease will disappear soon. Therefore, the density of infectious individuals at the steady state is close to 0 when β is near β_c, and it is often assumed that $p_i^{AI} = \epsilon_i \ll 1$ as $t \to \infty$. By simplifying $q_i^A(t)$ and $q_i^U(t)$ in equation (2.2), their

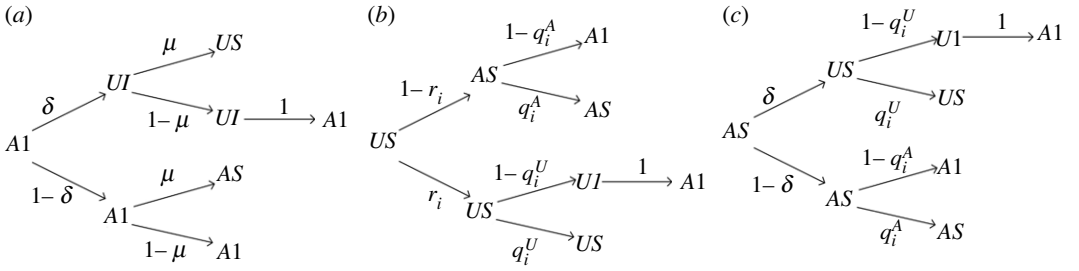

Figure 4. Transition probability trees for four states (*AS*, *AI*, *US*, *UI*). Individuals aware of epidemics will not be infected with probability $q_i^A(t)$, and individuals not aware of epidemics will not be infected with probability $q_i^U(t)$. $r_i(t)$ is used to denote the probability that an individual will not be informed by any neighbours who are aware of epidemics. δ means the probability that individuals aware of the information of epidemics may forget, and μ is the probability that infectious individuals may recover. It is assumed that the infectious individuals will become aware of epidemics spontaneously and become *AI* and thus *UI* is bound to become *AI* in the model.

values at the steady state can be calculated as follows:

$$\left.\begin{aligned} q_i^A &\approx 1-\beta^A\sum_j b_{ji}\epsilon_j \\ \text{and}\quad q_i^{UI} &\approx 1-\beta^U\sum_j b_{ji}\epsilon_j \end{aligned}\right\} \tag{2.6}$$

Inserting this approximate equality into equation (2.4), the following equations can be derived:

$$\left.\begin{aligned} p_i^{US} &= p_i^{US} r_i + p_i^{AS}\delta, \\ p_i^{AS} &= p_i^{US}(1-r_i) + p_i^{AS}(1-\delta) \\ \text{and}\quad \mu\epsilon_i &= (p_i^{AS}\beta^A + p_i^{US}\beta^U)\sum_j b_{ji}\epsilon_j. \end{aligned}\right\} \tag{2.7}$$

Then, the third equation in equation (2.7) can be further simplified by its first two equations as follows:

$$\sum_j[(1-(1-\gamma)p_i^A)b_{ji} - \frac{\mu}{\beta^U}\delta_{ji}]\epsilon_j = 0, \tag{2.8}$$

where δ_{ij} is the element of the identity matrix. Noting that the solution to equation (2.8) is an eigenvalue problem for the matrix H whose elements are $h_{ji} = (1-(1-\gamma)p_i^A)b_{ji}$. Then, the critical threshold of the proposed model can be obtained as follows:

$$\beta_c^U = \frac{\mu}{\Lambda_{\max}(H)}, \tag{2.9}$$

where $\Lambda_{\max}(H)$ is used to denote the maximum eigenvalue of matrix H. Henceforth, it is concluded that, according to equations (2.8) and (2.9), the epidemic threshold is related to the information diffusion in the upper virtual layer, especially to p_i^A. Furthermore, the topological structure of the lower physical layer, the values of μ and γ are also associated with the critical threshold of the epidemic model.

3. Monte Carlo simulation results

Firstly, ρ^I and ρ^A are depicted as a function of β in figures 5, 6 and 7, in which ρ^I is used to denote the density of infectious individuals at the steady state in the lower layer, ρ^A is adopted to express the density of individuals who are aware of the information about the disease at the steady state in the upper layer. In all simulations, the total number of nodes in each layer is assumed to be

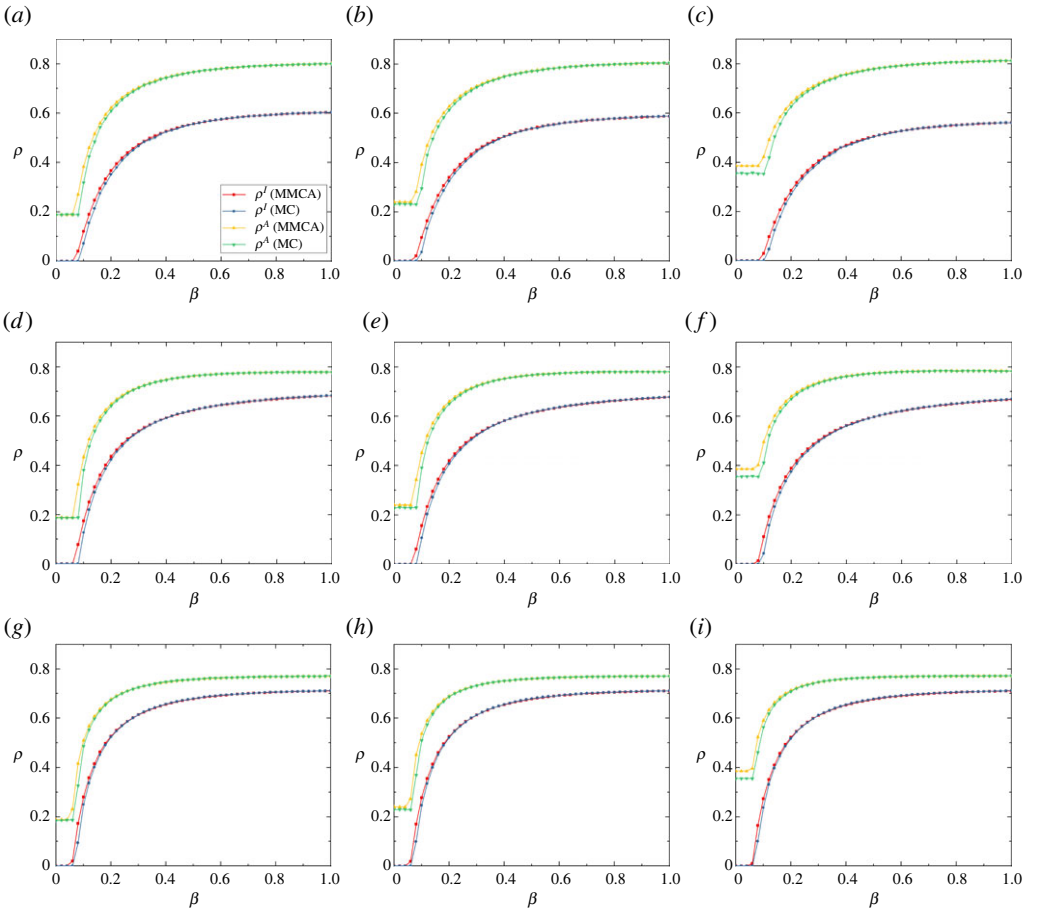

Figure 5. Densities of infectious individuals (ρ^I) and agents aware of epidemics (ρ^A) obtained by MMC approach and MC simulations with the increase of β, in which the yellow triangle line shows results of $\rho^I(MMC)$ and the green inverted triangle shows results of $\rho^I(MC)$. The red square line shows results of $\rho^A(MMC)$ and the blue circle line shows results of $\rho^A(MC)$. In panels (*a–c*), $\gamma = 0$, while $\gamma = 0.3$ in panels (*d–f*), and γ is set to be 0.9 in panels (*g–i*). At the same time, in panels (*a*), (*d*) and (*g*), $\lambda_\delta = 0$, while λ_δ is 0.6 in panels (*b*), (*e*) and (*h*), and λ_δ is set to be 2.4 in panels (*c*), (*f*) and (*i*). All the results of MC simulations are averaged over 50 independent runs and $\lambda = 0.1$. β is ranged from 0 to 1 with the step length of 0.02 including 0 and 1. (Online version in colour.)

$N = 1000$. All the upper networks are constructed by using random simplicial complexes [27], while all the lower networks are generated by the ER model [51], in which the probability of connection between any two nodes is 0.006. In addition, the initial value of ρ^I is equal to 1%, and other parameters are initialized to be $\delta = 0.8$, $\mu = 0.4$, $\gamma = 0$, $k_1 = 10$, $k_2 = 2$. According to equation (2.3), when $\lambda_\delta = 0$, $\lambda^* = 0$, when $\lambda_\delta = 0.6$, $\lambda^* \approx 0.2276$, when $\lambda_\delta = 2.4$, $\lambda^* \approx 0.9104$. The relative error of results obtained by MMC approach and MC simulations for infectious individuals with a group of parameters, such as λ, β, γ and so on, is calculated by $(|\rho^I_{\mathrm{MMC}} - \rho^I_{\mathrm{MC}}|/\rho^I_{\mathrm{MC}})$. By adding all the relative errors of k different groups of parameters and dividing it by k, the relative error of these k groups of parameters is derived. The relative errors for ρ^A are calculated in a similar way. Parameters and methods used in the following experiments are consistent with the above-mentioned ones if not specifically stated.

When the information transmission rate is set to be 0.1, the densities of aware individuals and infectious individuals at the steady state obtained by the MMC approach and MC simulations are shown in figure 5. In panel (*b*), the relative errors of ρ^I obtained by the MMC approach and MC

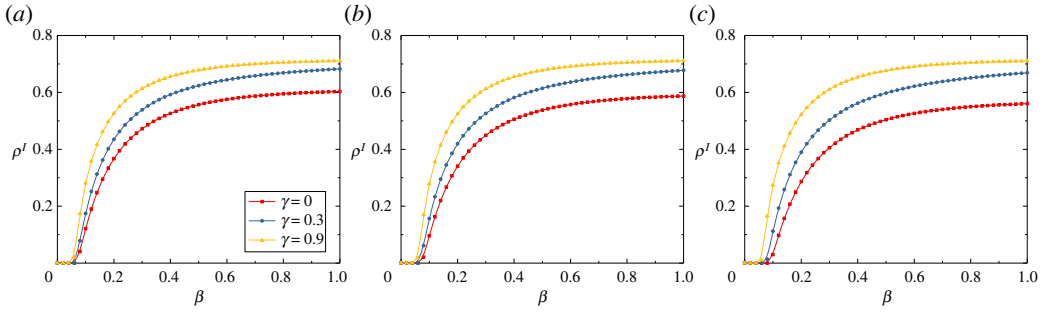

Figure 6. Density of infectious individuals (ρ^I) obtained by the MMC approach as a function of the disease transmission rate (β) at the steady state for different λ_δ and γ. In panel (*a*), $\lambda_\delta = 0$, the information transmission rate of 2-simplex (λ^*) is 0. In panel (*b*), $\lambda_\delta = 0.6$, $\lambda^* \approx 0.23$. In panel (*c*), $\lambda_\delta = 2.4$, $\lambda^* \approx 0.91$. The information transmission rate (λ) is 0.1 and β is ranged from 0 to 1 with the step length of 0.02 including 0 and 1. The loss rate of information (δ) is assumed to be 0.8. The recovery rate of disease (μ) is 0.4, $k_1 = 10$, $k_2 = 2$, $N = 1000$. The upper network is constructed with random simplicial complexes and the lower network is generated by the ER model. The red squares denote ρ^I with $\gamma = 0$, which means individuals who are aware of the disease cannot be infected. The blue circles and yellow triangles stand for ρ^I with $\gamma = 0.3$ and 0.9, respectively. (Online version in colour.)

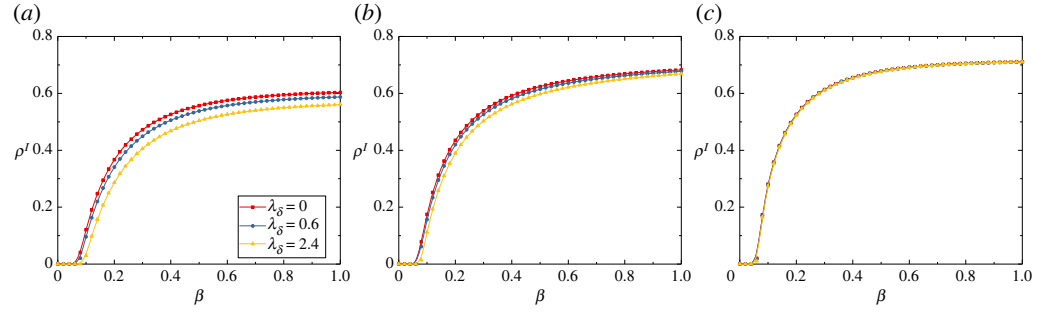

Figure 7. Density of infectious individuals (ρ^I) obtained by MMC approach as a function of the disease transmission rate (β) at the steady state in different λ_δ and γ. In panel (*a*), $\gamma = 0$, which means individuals who are aware of the disease cannot be infected directly. In panel (*b*), $\gamma = 0.3$. In panel (*c*), $\gamma = 0.9$. The information transmission rate (λ) is 0.1 and β is ranged from 0 to 1 with the step length of 0.02 including 0 and 1. The loss rate of information (δ) is 0.8. The recovery rate of disease (μ) is 0.4, $k_1 = 10$, $k_2 = 2$, $N = 1000$. The upper network is constructed with random simplicial complexes and the lower network is generated by ER model. The red squares represent ρ^I with $\lambda_\delta = 0$, $\lambda^* = 0$, which means the information transmission rate of 2-simplex is 0. The blue circles and yellow triangles denote ρ^I with $\lambda_\delta = 0.6$ ($\lambda^* \approx 0.23$) and 2.4($\lambda^* \approx 0.91$), respectively. (Online version in colour.)

simulations are around 5.83%, and they are around 4.32% in panel (*c*). In all the other panels of figure 5, the relative errors of ρ^I and ρ^A obtained by the MMC approach and MC simulations are around 2%. In panels (*a*), (*d*) and (*g*), $\lambda_\delta = 0$, $\lambda^* = 0$, at this time, the upper layer network is not affected by the 2-simplex, and information can only be propagated by the pairwise interaction among nodes. Overall, it is discovered that the relative errors are very small for different λ_δ, and the error is mainly generated around the threshold critical point. When $\beta > \beta_c$, the epidemics will tend to be endemic, and hence the density of infectious individuals will climb up quickly. However, the epidemics will quickly become extinct when $\beta < \beta_c$. Taken together, when the information transmission rate is set to be 0.1, the results obtained by the MMC approach well agree with these obtained by MC simulations, which demonstrates that the proposed model can be predicted accurately.

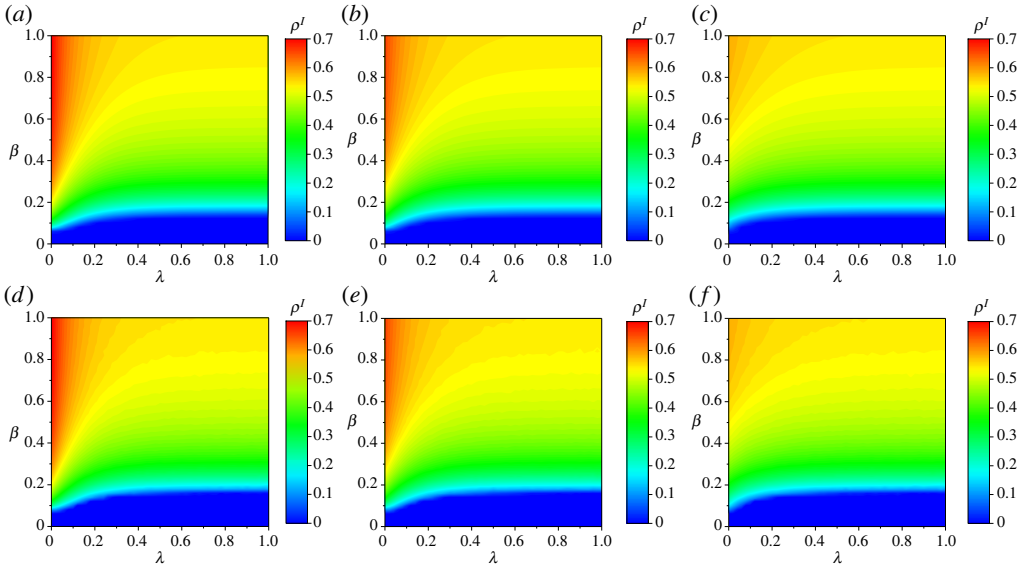

Figure 8. Densities of infectious individuals (ρ^I) as a function of β and λ at the steady state by MMC approach and MC simulations. Panels (*a–c*) are results obtained by the MMC approach. Panels (*d–f*) are results obtained by MC simulations. In panels (*a*) and (*d*), $\lambda_\delta = 0$. In panels (*b*,*e*), $\lambda_\delta = 0.6$. In panels (*c*,*f*), $\lambda_\delta = 2.4$. $\gamma = 0$. All results of MC simulations are obtained by averaging 50 independent runs. The colours of each panel mean the density of ρ^I for each point within a grid of 50∗50. (Online version in colour.)

To reveal the influence of different γ and λ_δ, the densities of infectious individuals obtained by the MMC approach are pictured in figures 6 and 7. It is discovered that ρ^I increases as γ increases. When $1 > \gamma > 0$, it means some of susceptible individuals who are aware of the disease would not take measures to reduce their risk of being infected, or the measures they take are not able to protect them from the disease effectively, which leads to the situation where the density of infectious individuals arises eventually. At the same time, it is found that the effect of λ_δ is limited when $\gamma > 0$, especially for the case under $\gamma = 0.9$ (figure 7*c*).

In order to further investigate the impact of λ and β, the results obtained by the MMC approach and MC simulations are pictured in figure 8. In panels (*a*,*d*), $\lambda_\delta = 0$, $\lambda^* = 0$ and the relative error is around 6.56%; in panels (*b*,*e*), $\lambda_\delta = 0.6$, $\lambda^* \approx 0.2276$, and the relative error is about 6.11%; in panels (*c*,*f*), $\lambda_\delta = 2.4$, $\lambda^* \approx 0.9104$, and the relative error is only 6.91%. All these results indicate that the relative errors between the MMC approach and MC simulations are small enough. In particular, it is also found that, when λ is small ($0 < \lambda < 0.3$) and β ($0.4 < \beta < 1$) is large, ρ^I decreases as λ_δ increases, especially when $\lambda_\delta = 2.4$, ρ^I is the smallest one. When β is larger and λ is smaller, the infectious disease spreads widely throughout the network, but the spread of information is weak. Increasing λ_δ can increase λ^* and promote the spread of information on the 2-simplex, which in turn drives the diffusion of information related to the infectious disease throughout the upper network, then corresponding nodes take certain measures to reduce their risk of being infected, and thus the overall density of infectious individuals will decrease. This phenomenon implies that increasing λ_δ can inhibit the spread of infectious diseases when β is larger and λ is smaller. But when λ is larger ($\lambda > 0.3$), the density of infectious nodes would not decrease as λ_δ increases, since the whole network has reached the stable state at this time, and neither increasing λ nor λ_δ can reduce the density of infectious nodes.

Henceforth, it is discovered that λ and λ_δ can interact with each other and commonly influence the propagation of information in the network. In particular, the effect of information diffusion rate of 2-simplex becomes more obvious when β is large and λ is small.

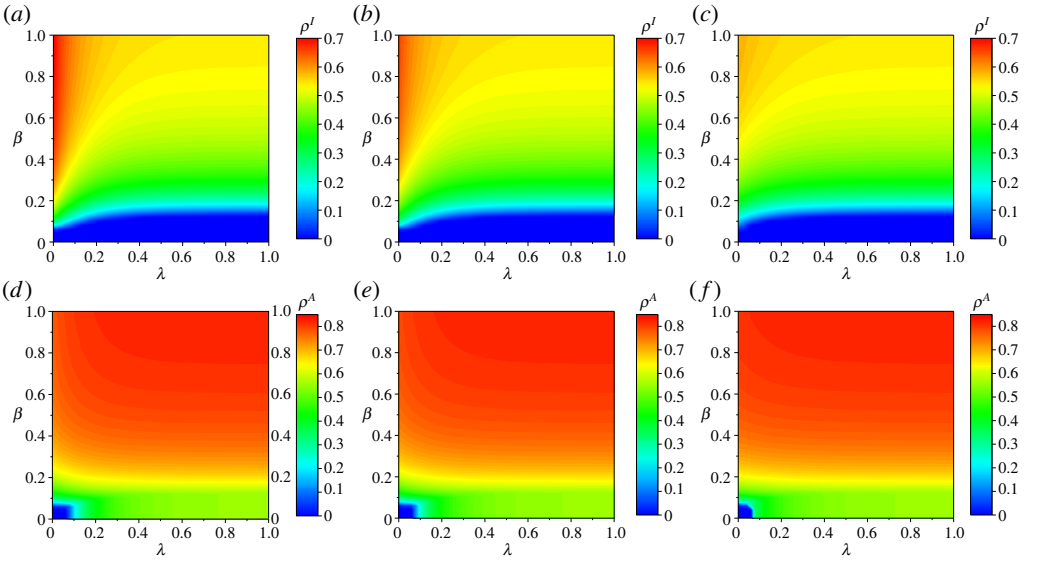

Figure 9. Densities of infectious individuals (ρ^I) and people aware of disease (ρ^A) as a function of β and λ at the steady state by MMC approach. Panels (*a*–c) are densities of infectious individuals. Panels (*d*–*f*) denote the densities of agents aware of disease. In panels (*a*) and (*d*), $\lambda_\delta = 0$. While, in panels (*b*,*e*), $\lambda_\delta = 0.6$. In panels (*c*,*f*), $\lambda_\delta = 2.4$. $\gamma = 0$. All results of MC simulations are attained by averaging 50 independent realizations. The colours of each panel mean the density for each point within a grid of 50∗50. (Online version in colour.)

The density of infectious individuals (ρ^I) and density of agents aware of disease (ρ^A) at the steady state obtained by the MMC approach are illustrated in figure 9. By observing panels (*d*–*f*), it is discovered that ρ^A gradually increases with the increase of λ_δ in the region where β is larger and λ is smaller, while it tends to be stable when λ is larger. This coincides with the previously drawn conclusion since the propagation of information on the 2-simplex will be promoted by increasing λ_δ when β is large and λ is small. The propagation of information in the upper network would be facilitated in turn. Therefore, the density of agents aware of disease increases. When λ is larger, the density of individuals in the whole network that know the information of infectious diseases has reached the saturation, and there is no effect even if λ_δ is increased further. By observing panels (*a*–*c*), it can be found that ρ^I gradually decreases with the increase of λ_δ in the region where β is larger and λ is smaller. It has been assumed that the *UI* state is directly transformed to the *AI* state and *AS* state nodes cannot be directly infected, so the total number of nodes in the *AI* state is equal to the total number of nodes in the *I* state, while the total number of nodes in the *A* state is equal to the total number of nodes in the *AI* state plus the total number of nodes in the *AS* state. It is also concluded that, by increasing λ_δ, when β is larger and λ is smaller, the density of *AI* state nodes decreases but the density of *A* state nodes increases, which means that the number of *AS* state nodes in panels (*b*,*f*) gradually accumulates, and the role of 2-simplex in promoting information dissemination is demonstrated, confirming the results obtained earlier again.

The critical threshold obtained by this model is shown in detail in figure 10. In panel (*a*), when $\gamma = 0$, it is shown that the epidemic threshold increases as λ_δ increases when $0.05 < \lambda < 0.4$, and it would not be increased by increasing λ_δ when $\lambda \geq 0.4$. In panel (*b*), when $\gamma = 0.3$, the thresholds of different λ_δ are definitely smaller than these of $\gamma = 0$ when $0.05 < \lambda < 0.4$. It is apparent that increasing λ_δ, which increases the propagation of information on 2-simplex, can increase the threshold to some extent and make the outbreak of infectious diseases more difficult. But the effect of λ_δ decreases as γ increases, which demonstrates the inhibitory effect of λ_δ on epidemic propagation is limited.

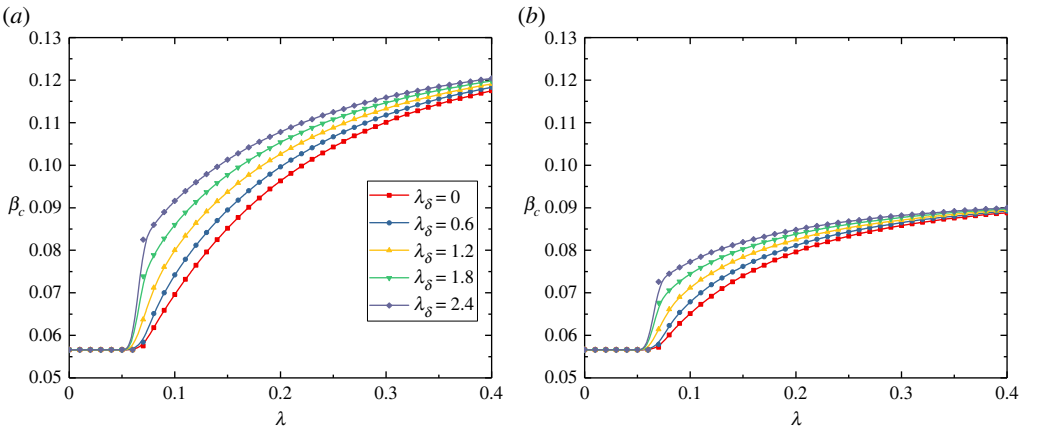

Figure 10. Epidemic threshold (β_c) obtained by the MMC approach as a function of the information transmission rate (λ) in different λ_δ and γ. λ takes the values from 0 to 0.4 with the step length of 0.01 including 0 and 0.4. In panel (*a*), γ is set to be 0, which means people aware of the epidemic would not be infected. In panel (*b*), γ is set to be 0.3. The loss rate of information (δ) is assumed to be 0.8. The recovery rate of disease (μ) is 0.4, $k_1 = 10$, $k_2 = 2$, $N = 1000$. The upper network is constructed with random simplicial complexes and the lower network is generated by ER model. The red squares denote β_c with $\lambda_\delta = 0$ and $\lambda^* = 0$, which means the information transmission rate of 2-simplex is 0. The blue circles and yellow upper triangles indicate β_c with $\lambda_\delta = 0.6(\lambda^* \approx 0.23)$ and $1.2(\lambda^* \approx 0.46)$, respectively. The green lower triangles and grey squares stand for β_c with $\lambda_\delta = 1.8$ ($\lambda^* \approx 0.69$) and $2.4(\lambda^* \approx 0.91)$, respectively. (Online version in colour.)

Therefore, increasing λ_δ can enlarge the epidemic threshold to some extent, especially for the lower γ, and it affects the threshold by controlling the propagation of information in the 2-simplex through λ^*. This interaction mechanism is similar to the impact of λ on the threshold and thus it is an indirect effect.

4. Discussion

In summary, a new epidemic model on the two-layered network to illustrate the coupling spread between epidemics and information is proposed in this paper, where the upper layer denotes the virtual contact network constructed with random simplicial complexes and the lower layer stands for the physical contact network. At first, the MMC approach is adopted to construct probability transition equations to analyse the outbreak threshold of infectious diseases. Then, the average densities of infectious individuals and those knowing the information of infectious disease at steady state were obtained by multiple MC simulations. The results derived by the MMC approach and MC simulations are found to be matched well after detailed comparisons, indicating that this new model can be well predicted. The main results are as follows:

— 2-simplex provides the extra possibility for an individual to be informed, and thus the information transmission on the information layer can be promoted by increasing the information transmission rate, especially when the disease transmission rate is high and the information transmission rate is low.
— Information transmission induced by the 2-simplex can further increase the threshold of disease outbreak and suppress its outbreak to a certain extent, but this impact decreases as γ increases.

Although concepts related to higher-order interactions have been proposed in mathematics for a long time, studies associating them with complex network are still in their infancy. Thus, exploring the impact of higher-order interactions on the dynamics on top of networks deserves

much more attention. Specifically, in the area of coupling propagation between information and epidemics, when the dissemination of information includes not only local information, but also contact information and global information, corresponding networks constructed with simplicial complexes or hypergraphs may induce the diverse phenomena. Meanwhile, when information spreading is not limited to pairwise interaction, but extended to herd-like contagion, the introduction of simplicial complexes or hypergraphs may also create some unexpected phenomena. Meanwhile, in our opinion, integrating the higher-order interactions with multilayer or interdependent networks may provide a potential means to illustrate the relationship between the network structure and dynamics taking place upon them.

Taken together, the current results are highly enlightening, and the role of simplicial complexes in the transmission of information or disease should be taken into account, which would help public health authorities to better design effective measures to deal with possible future outbreaks of epidemics or even pandemics.

Acknowledgements. M.P. acknowledges the funding from the Slovenian Research Agency (grant nos. P1-0403 and J1-2457).

Data accessibility. The code used in the study is available at: https://github.com/fjf-git/simplicial_complex/tree/epidemics-on-multilayer-simplicial-complexes.

Authors' contributions. J.F.: data curation, formal analysis, investigation, software, visualization, writing—original draft; Q.Y.: data curation, formal analysis, investigation, methodology, resources, visualization, writing—original draft; C.X.: conceptualization, investigation, project administration, supervision, validation, writing—original draft, writing—review and editing; M.P.: conceptualization, funding acquisition, supervision, writing—original draft, writing—review and editing.

All authors gave final approval for publication and agreed to be held accountable for the work performed therein.

Conflict of interest declaration. We declare we have no competing interests.

Funding. C.X. is supported by the National Natural Science Foundation of China (grant no. 62173247). M.P. is supported by the Slovenian Research Agency (grant nos. P1-0403 and J1-2457).

References

1. Strogatz SH. 2001 Exploring complex networks. *Nature* **410**, 268–276. (doi:10.1038/35065725)
2. Newman MEJ. 2003 The structure and function of complex networks. *SIAM Rev.* **45**, 167–256. (doi:10.1137/S003614450342480)
3. Boccaletti S, Latora V, Moreno Y, Chavez M, Hwang DU. 2006 Complex networks: structure and dynamics. *Phys. Rep.* **424**, 175–308. (doi:10.1016/j.physrep.2005.10.009)
4. Kashyap G, Bapat D, Das D, Gowaikar R, Amritkar RE, Rangarajan G, Ravindranath V, Ambika G. 2019 Synapse loss and progress of Alzheimer's disease-A network model. *Sci. Rep.* **9**, 1–9. (doi:10.1038/s41598-019-43076-y)
5. Resmi V, Ambika G, Amritkar RE, Rangarajan G. 2012 Amplitude death in complex networks induced by environment. *Phys. Rev. E* **85**, 046211. (doi:10.1103/PhysRevE.85.046211)
6. Buldyrev SV, Parshani R, Paul G, Stanley HE, Havlin S. 2010 Catastrophic cascade of failures in interdependent networks. *Nature* **464**, 1025–1028. (doi:10.1038/nature08932)
7. Wang Z, Wang L, Szolnoki A, Perc M. 2015 Evolutionary games on multilayer networks: a colloquium. *Eur. Phys. J. B* **88**, 1–15.
8. Sun H, Bianconi G. 2021 Higher-order percolation processes on multiplex hypergraphs. *Phys. Rev. E* **104**, 034306. (doi:10.1103/PhysRevE.104.034306)
9. Su Q, McAvoy A, Mori Y, Plotkin JB. 2022 Evolution of prosocial behaviours in multilayer populations. *Nat. Hum. Behav.* **6**, 1–11. (doi:10.1038/s41562-022-01299-6)
10. Su Q, McAvoy A, Plotkin JB. 2022 Evolution of cooperation with contextualized behavior. *Sci. Adv.* **8**, eabm6066.
11. Boccaletti S, Bianconi G, Criado R, Del Genio CI, Gómez-Gardeñes J, Romance M, Sendiña-Nadal I, Wang Z, Zanin M. 2014 The structure and dynamics of multilayer networks. *Phys. Rep.* **544**, 1–122. (doi:10.1016/j.physrep.2014.07.001)
12. Kivelä M, Arenas A, Barthelemy M, Gleeson JP, Moreno Y, Porter MA. 2014 Multilayer networks. *J. Complex Networks* **2**, 203–271. (doi:10.1093/comnet/cnu016)

13. Gómez S, Diaz-Guilera A, Gómez-Gardeñes J, Perez-Vicente CJ, Moreno Y, Arenas A. 2013 Diffusion dynamics on multiplex networks. *Phys. Rev. Lett.* **110**, 028701. (doi:10.1103/PhysRevLett.110.028701)
14. De Domenico M, Solé-Ribalta A, Cozzo E, Kivelä M, Moreno Y, Porter MA, Gómez S, Arenas A. 2013 Mathematical formulation of multilayer networks. *Phys. Rev. X* **3**, 041022. (doi:10.1103/PhysRevX.3.041022)
15. De Domenico M, Granell C, Porter MA, Arenas A. 2016 The physics of spreading processes in multilayer networks. *Nat. Phys.* **12**, 901–906. (doi:10.1038/nphys3865)
16. Wang W, Tang M, Yang H, Do Y, Lai YC, Lee G. 2014 Asymmetrically interacting spreading dynamics on complex layered networks. *Sci. Rep.* **4**, 1–8. (doi:10.1038/srep05097)
17. Pastor-Satorras R, Castellano C, Van Mieghem P, Vespignani A. 2015 Epidemic processes in complex networks. *Rev. Mod. Phys.* **87**, 925. (doi:10.1103/RevModPhys.87.925)
18. Wang W, Liu QH, Cai SM, Tang M, Braunstein LA, Stanley HE. 2016 Suppressing disease spreading by using information diffusion on multiplex networks. *Sci. Rep.* **6**, 1–14. (doi:10.1038/s41598-016-0001-8)
19. Liu QH, Wang W, Tang M, Zhang HF. 2016 Impacts of complex behavioral responses on asymmetric interacting spreading dynamics in multiplex networks. *Sci. Rep.* **6**, 1–13. (doi:10.1038/s41598-016-0001-8)
20. Granell C, Gómez S, Arenas A. 2013 Dynamical interplay between awareness and epidemic spreading in multiplex networks. *Phys. Rev. Lett.* **111**, 128701. (doi:10.1103/PhysRevLett.111.128701)
21. Granell C, Gómez S, Arenas A. 2014 Competing spreading processes on multiplex networks: awareness and epidemics. *Phys. Rev. E* **90**, 012808. (doi:10.1103/PhysRevE.90.012808)
22. Guo QT, Jiang X, Lei Y, Li M, Ma Y, Zheng ZM. 2015 Two-stage effects of awareness cascade on epidemic spreading in multiplex networks. *Phys. Rev. E* **91**, 012822. (doi:10.1103/PhysRevE.91.012822)
23. Guilbeault D, Becker J, Centola D. 2018 Complex contagions: a decade in review. In *Complex Spreading Phenomena in Social Systems* (eds S Lehmann, Y-Y Ahn), pp. 3–25. Cham, Switzerland: Springer.
24. Karsai M, Iñiguez G, Kaski K, Kertész J. 2014 Complex contagion process in spreading of online innovation. *J. R. Soc. Interface* **11**, 20140694. (doi:10.1098/rsif.2014.0694)
25. Mønsted B, Sapieżyński P, Ferrara E, Lehmann S. 2017 Evidence of complex contagion of information in social media: an experiment using Twitter bots. *PLoS ONE* **12**, e0184148. (doi:10.1371/journal.pone.0184148)
26. Wang W, Liu QH, Liang J, Hu Y, Zhou T. 2019 Coevolution spreading in complex networks. *Phys. Rep.* **820**, 1–51. (doi:10.1016/j.physrep.2019.07.001)
27. Iacopini I, Petri G, Barrat A, Latora V. 2019 Simplicial models of social contagion. *Nat. Commun.* **10**, 1–9. (doi:10.1038/s41467-019-10431-6)
28. Alvarez-Rodriguez U, Battiston F, de Arruda GF, Moreno Y, Perc M, Latora V. 2021 Evolutionary dynamics of higher-order interactions in social networks. *Nat. Hum. Behav.* **5**, 586–595. (doi:10.1038/s41562-020-01024-1)
29. Cook SJ *et al.* 2019 Whole-animal connectomes of both Caenorhabditis elegans sexes. *Nature* **571**, 63–71. (doi:10.1038/s41586-019-1352-7)
30. Sizemore AE, Giusti C, Kahn A, Vettel JM, Betzel RF, Bassett DS. 2018 Cliques and cavities in the human connectome. *J. Comput. Neurosci.* **44**, 115–145. (doi:10.1007/s10827-017-0672-6)
31. Reimann MW *et al.* 2017 Cliques of neurons bound into cavities provide a missing link between structure and function. *Front. Comput. Neurosci.* **11**, 48. (doi:10.3389/fncom.2017.00048)
32. Mayfield MM, Stouffer DB. 2017 Higher-order interactions capture unexplained complexity in diverse communities. *Nat. Ecol. Evol.* **1**, 1–7. (doi:10.1038/s41559-016-0062)
33. Bairey E, Kelsic ED, Kishony R. 2016 High-order species interactions shape ecosystem diversity. *Nat. Commun.* **7**, 1–7. (doi:10.1038/ncomms12285)
34. Grilli J, Barabás G, Michalska-Smith MJ, Allesina S. 2017 Higher-order interactions stabilize dynamics in competitive network models. *Nature* **548**, 210–213. (doi:10.1038/nature23273)
35. Torres L, Blevins AS, Bassett D, Eliassi-Rad T. 2021 The why, how, and when of representations for complex systems. *SIAM Rev.* **63**, 435–485. (doi:10.1137/20M1355896)
36. Patania A, Vaccarino F, Petri G. 2017 Topological analysis of data. *Europhys. J. Data Sci.* **6**, 1–6. (doi:10.1140/epjds/s13688-016-0097-x)

37. Benson AR, Gleich DF, Leskovec J. 2016 Higher-order organization of complex networks. *Science* **353**, 163–166. (doi:10.1126/science.aad9029)
38. Battiston F, Cencetti G, Iacopini I, Latora V, Lucas M, Patania A, Young JG, Petri G. 2020 Networks beyond pairwise interactions: structure and dynamics. *Phys. Rep.* **874**, 1–92. (doi:10.1016/j.physrep.2020.05.004)
39. Matamalas JT, Gómez S, Arenas A. 2020 Abrupt phase transition of epidemic spreading in simplicial complexes. *Phys. Rev. Res.* **2**, 012049. (doi:10.1103/PhysRevResearch.2.012049)
40. Cisneros-Velarde P, Bullo F. 2021 Multi-group SIS epidemics with simplicial and higher-order interactions. *IEEE Trans. Control Netw. Syst.* (doi:10.1109/TCNS.2021.3124269)
41. Neuhäuser L, Mellor A, Lambiotte R. 2020 Multibody interactions and nonlinear consensus dynamics on networked systems. *Phys. Rev. E* **101**, 032310. (doi:10.1103/PhysRevE.101.032310)
42. Chodrow PS. 2020 Configuration models of random hypergraphs. *J. Complex Networks* **8**, cnaa018. (doi:10.1093/comnet/cnaa018)
43. Courtney OT, Bianconi G. 2017 Weighted growing simplicial complexes. *Phys. Rev. E* **95**, 062301. (doi:10.1103/PhysRevE.95.062301)
44. Salnikov V, Cassese D, Lambiotte R. 2018 Simplicial complexes and complex systems. *Eur. J. Phys.* **40**, 014001. (doi:10.1088/1361-6404/aae790)
45. Battiston F *et al.* 2021 The physics of higher-order interactions in complex systems. *Nat. Phys.* **17**, 1093–1098. (doi:10.1038/s41567-021-01371-4)
46. Petri G, Barrat A. 2018 Simplicial activity driven model. *Phys. Rev. Lett.* **121**, 228301. (doi:10.1103/PhysRevLett.121.228301)
47. Lambiotte R, Rosvall M, Scholtes I. 2019 From networks to optimal higher-order models of complex systems. *Nat. Phys.* **15**, 313–320. (doi:10.1038/s41567-019-0459-y)
48. Peña J, Wu B, Arranz J, Traulsen A. 2016 Evolutionary games of multiplayer cooperation on graphs. *PLoS Comput. Biol.* **12**, e1005059. (doi:10.1371/journal.pcbi.1005059)
49. Su Q, Zhou L, Wang L. 2019 Evolutionary multiplayer games on graphs with edge diversity. *PLoS Comput. Biol.* **15**, e1006947. (doi:10.1371/journal.pcbi.1006947)
50. de Arruda GF, Petri G, Rodriguez PM, Moreno Y. 2021 Multistability, intermittency and hybrid transitions in social contagion models on hypergraphs. (http://arxiv.org/abs/2112.04273).
51. Erdös P, Rényi A. 1960 On the evolution of random graphs. *Publ. Math. Inst. Hung. Acad. Sci.* **5**, 17–60.